

Preliminary Results of Radar Environmental Mapping

B. H. CANTRELL

*Radar Analysis Staff
Radar Division*

April 28, 1980



NAVAL RESEARCH LABORATORY
Washington, D.C.

Approved for public release; distribution unlimited.

REPORT DOCUMENTATION PAGE		READ INSTRUCTIONS BEFORE COMPLETING FORM								
1. REPORT NUMBER NRL Report 8400	2. GOVT ACCESSION NO.	3. RECIPIENT'S CATALOG NUMBER								
4. TITLE (and Subtitle) PRELIMINARY RESULTS OF RADAR ENVIRONMENTAL MAPPING		5. TYPE OF REPORT & PERIOD COVERED Interim report on a continuing NRL problem number								
		6. PERFORMING ORG. REPORT NUMBER								
7. AUTHOR(s) B. H. Cantrell		8. CONTRACT OR GRANT NUMBER(s)								
9. PERFORMING ORGANIZATION NAME AND ADDRESS Naval Research Laboratory Washington, DC 20375		10. PROGRAM ELEMENT, PROJECT, TASK AREA & WORK UNIT NUMBERS 61153N; RR-021-05-41; NRL Problem 53-0628-0								
11. CONTROLLING OFFICE NAME AND ADDRESS Department of the Navy Office of Naval Research Arlington, VA 22217		12. REPORT DATE April 28, 1980								
		13. NUMBER OF PAGES 20								
14. MONITORING AGENCY NAME & ADDRESS (if different from Controlling Office)		15. SECURITY CLASS. (of this report) UNCLASSIFIED								
		15a. DECLASSIFICATION/DOWNGRADING SCHEDULE								
16. DISTRIBUTION STATEMENT (of this Report) Approved for public release; distribution unlimited.										
17. DISTRIBUTION STATEMENT (of the abstract entered in Block 20, if different from Report)										
18. SUPPLEMENTARY NOTES										
19. KEY WORDS (Continue on reverse side if necessary and identify by block number)										
<table> <tbody> <tr> <td>Detectors</td> <td>Clutter</td> </tr> <tr> <td>Radars</td> <td>Noise</td> </tr> <tr> <td>Estimation</td> <td>Interference</td> </tr> <tr> <td>Radar echoes</td> <td>Radar mapping</td> </tr> </tbody> </table>			Detectors	Clutter	Radars	Noise	Estimation	Interference	Radar echoes	Radar mapping
Detectors	Clutter									
Radars	Noise									
Estimation	Interference									
Radar echoes	Radar mapping									
20. ABSTRACT (Continue on reverse side if necessary and identify by block number)										
<p>The signals received by radars often contain much more information than the echoes from targets, but usually only the target echoes are extracted. Means of extracting the environmental conditions such as rain and land clutter, noise jamming, short-pulse interference, and thermal-noise regions are studied. The knowledge of the environmental conditions is thought to be useful in target tracking and radar control processes.</p>										

CONTENTS

INTRODUCTION	1
PRINCIPLES OF OPERATION	2
QUALITATIVE RESULTS	11
SUMMARY	14
ACKNOWLEDGMENTS	18
REFERENCES	18

PRELIMINARY RESULTS OF RADAR ENVIRONMENTAL MAPPING

INTRODUCTION

The detection of radar echoes from targets has received a lot of attention through the years. A large body of theory has been developed and is represented in textbooks and in more recent articles. Far from being of only theoretical interest, considerable operational as well as experimental equipment exists and is used to enhance or to detect radar echos from targets such as aircraft, missiles, and ships. Thus far the major emphasis to date in detection and signal processing has been to remove all extraneous signals and provide detection mechanisms for targets. However, another useful endeavor could be to provide a means of describing the environmental conditions surrounding and underlying the target-detection regions. Of course the target detections would still remain of prime interest. The environmental map could supply badly needed information for improved operation of the tracking system, and because a better picture of the prevailing situation would be available, the detector or radar operation could be modified accordingly.

After this statement that environmental maps may be useful, the question which naturally arises is what constitutes an environmental map. As a rather general and vague description, a radar environmental map is a representation of events, things, and processes which can relate to the signals received and processed by the radar. Of course this description could mean many things to many people. Some examples of what may be of interest and included in the map are land masses, rain, receiver saturation, ducting conditions, in-band jamming, out-of-band jamming, types of jamming, measurement accuracies, thermal-noise-limited regions, multipath conditions, and sea clutter.

The following assumptions affect how this report will proceed. The radar does not have or does not use pulse-to-pulse coherence, so that doppler filtering is not performed. No spatial filtering in the sense of adaptive spatial null-forming circuits are used. The radar PRF is low, so that multiple time-around echos are not received. The radar is pulsed as opposed to CW or interrupted CW. Only the signals in the normal radar receiver passband are to be used. Of course this generic radar type is representative of most pulsed surveillance radars in operation in the world today. The environmental classifications considered are targets, land clutter, rain clutter, thermal-noise regions, shortpulse interference (at least as short as the radar's pulse), and noise jamming. Of course these types of echoes and sources are the most prevalent type of signals encountered by the generic radar postulated.

The material content of this work is further restricted to detection and classification of the signal type from range cell to range cell. The data in most cases would probably be of more use if the signal types could be classified over regions of space rather than from range cell to range cell. The probable procedure for classifying signal types over regions of space

CANTRELL

would be to define region boundaries based on the declaration of signal type from range cell to range cell described within this report. Consequently the regional classification naturally follows the work to be presented here and will be considered in future work.

Recordings of the video signals present on the SPS-12 and SPS-39 radars were made by Don Queen and Jim Alter of NRL and are used extensively throughout the report. The radars were at the Chesapeake Bay Division of NRL on top of building 75, which overlooks the bay. The SPS-12 is a 2D radar with a magnetron transmitter, an azimuth beamwidth of about 3° , a $1\text{-}\mu\text{s}$ pulse width, a rotation rate of 10 rpm, and a PRF of 500 pps. The SPS-39 was not operated in its normal mode. The pertinent parameters in the mode it was operated are 2D operation (single beam), an azimuth beamwidth of about 2° , a $2\text{-}\mu\text{s}$ pulse width, a rotation rate of 7.5 rpm, and a PRF of 500 pps. The video on the SPS-12 was sampled at a megahertz rate, and the video on the SPS-39 was sampled at a 500-kilohertz rate. The amplitude of the video at each sample was recorded and is called the amplitude sample at that range cell.

This report will proceed as follows. First the processing circuits will be described. Then, examples of the operation under different conditions will be shown. Finally the results will be given in a qualitative manner by observing the classifications displayed using a PPI (plan position indicator) format. The work to be described here was also described in a patent application [1].

PRINCIPLES OF OPERATION

The classes of signals which are present in the recorded data to be studied are interference, rain clutter, noise jamming, land clutter, isolated targets, and thermal noise. In the data to be studied the PRF is low enough so that the rain clutter is for all practical purposes decorrelated from pulse to pulse. Consequently, on a range-cell-to-range-cell basis it is indistinguishable from noise jamming, and the rain clutter and noise jamming are merged into one category. These could be later separated in that rain occurs in patches and the noise jamming occurs in azimuth strobos. However, this separation is not studied in this report.

The environmental-map circuit shown in Fig. 1 requires radar echoes from two identical successive pulses (at the same frequency) separated in time by several milliseconds. Given the two radar echoes, the environmental map decides from range cell to range cell the type of echo or interference which is present.

The circuit operation is briefly as follows: The echoes from the first pulse are stored until echoes from the second pulse are received. The first operation is to subtract the echoes from the same ranges, thus removing heavy correlated land and target returns, leaving only interference spikes and uncorrelated noise. The interference spikes are detected using a log cell-averaging CFAR (constant-false-alarm-rate) detector, and those range cells are declared interference. The range cells containing interference spikes are deleted from further use in the threshold calculations. The signals left after pulse-to-pulse subtraction and interference removal are now uncorrelated. The uncorrelated noise power in a local vicinity is compared to the thermal noise, and if it exceeds the thermal noise, either noise jamming or rain clutter is declared. Correlated signals above the local uncorrelated signal or noise background are

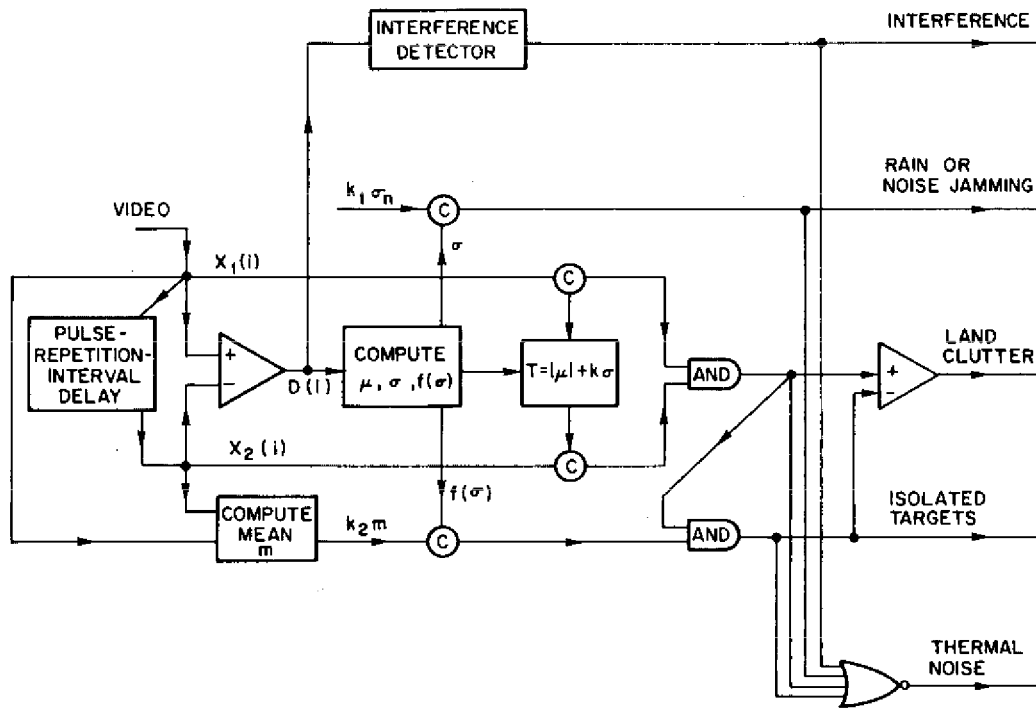


Fig. 1 — Processing circuit for an environmental map

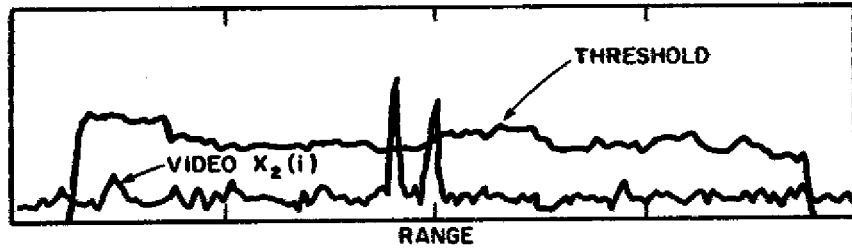
next detected. These are separated into two types, distributed land clutter and isolated targets, by accepting as targets only those correlated returns which are surrounded by a few range cells with uncorrelated echoes. Some isolated land-clutter returns will appear as targets but can be removed by noting they do not move with time. The last category, a thermal noise region, is declared when no other declarations are present.

A more detailed description is now given. In the processing that will be performed it is always assumed that the radar is pulsed twice at the same frequency, and the echoes, designated $X_1(i)$ and $X_2(i)$ respectively, are recorded versus range. Examples of these recordings are given in Figs. 2 through 6, parts a and b. Figures 2a and 2b show that thermal noise is present at all ranges except for two targets separated by a few range cells which are present near the center of the range interval. Given n range cells, the first operation shown in Fig. 1 is pulse-to-pulse subtraction given by

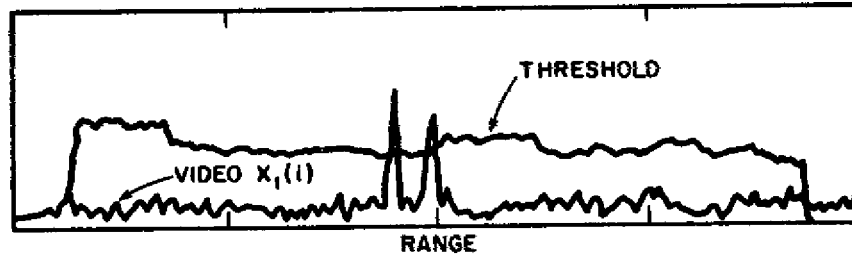
$$D(i) = X_1(i) - X_2(i)$$

for $i = 1, 2, \dots, n$. With use of the recorded data, the results for $\{D(i)\}$ are shown in part c of Figs. 2 through 6. The correlated targets and land clutter are removed from the data, leaving only noise which is directly related to Rayleigh-distributed thermal noise in the records of $X_1(i)$ and $X_2(i)$, as shown in Figs. 2c and 3c. In addition Figs. 4c and 5c show a noisy record for $\{D(i)\}$ whose standard deviation appears to be proportional to the standard

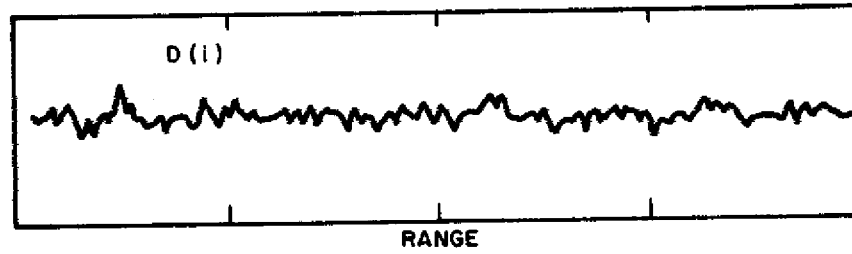
CANTRELL



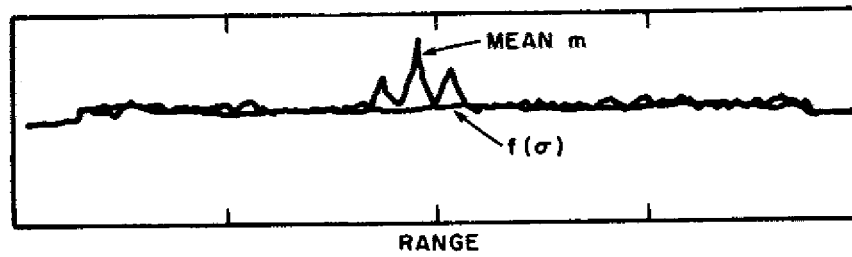
(a) Echo from pulse 1



(b) Echo from pulse 2

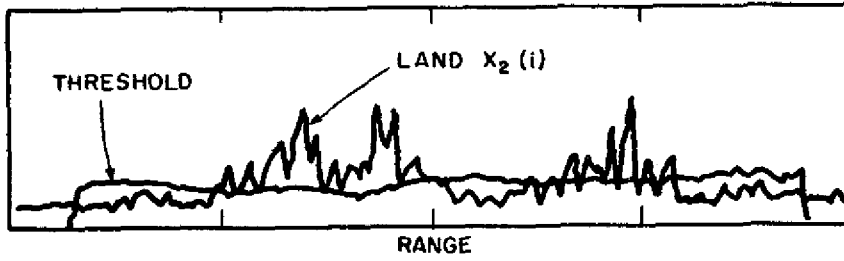


(c) Difference in echoes

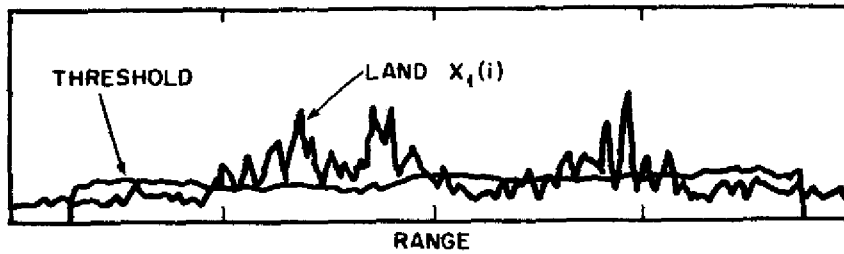


(d) Mean comparison

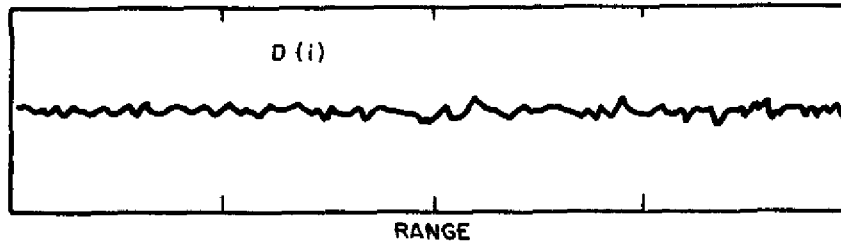
Fig. 2 — Two targets in noise



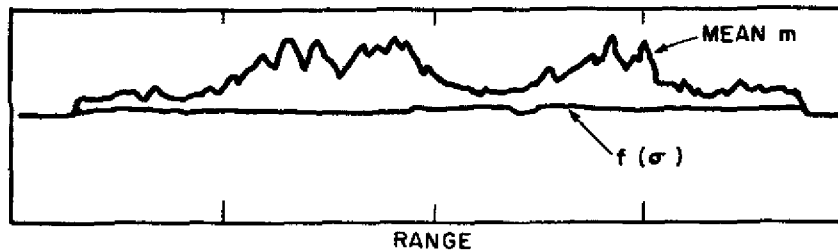
(a) Echo from pulse 1



(b) Echo from pulse 2

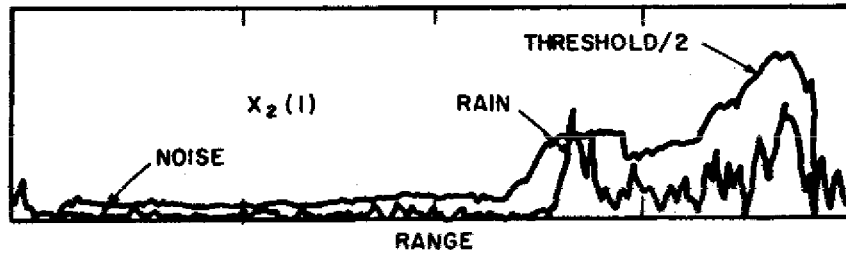


(c) Difference in echoes

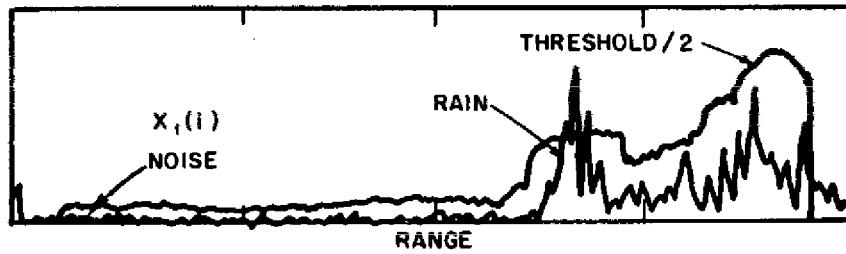


(d) Mean comparison

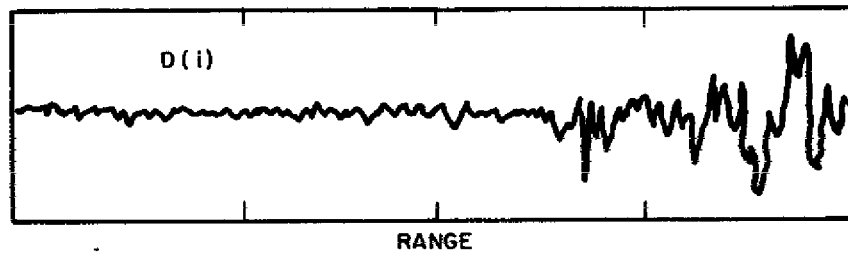
Fig. 3 — Land clutter



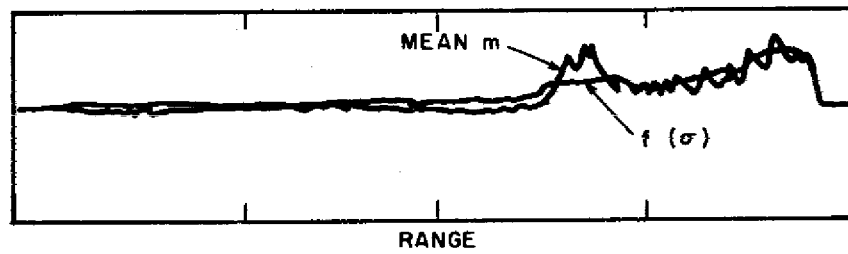
(a) Echo from pulse 1



(b) Echo from pulse 2

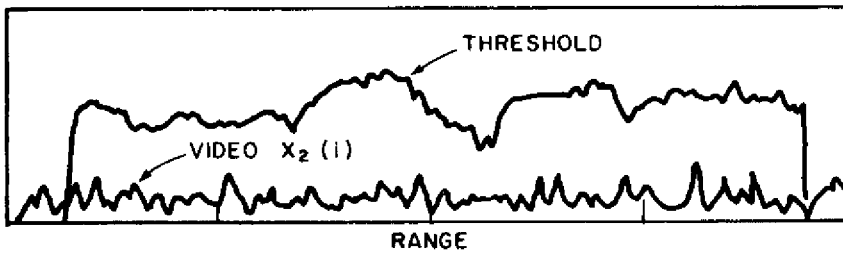


(c) Difference in echoes

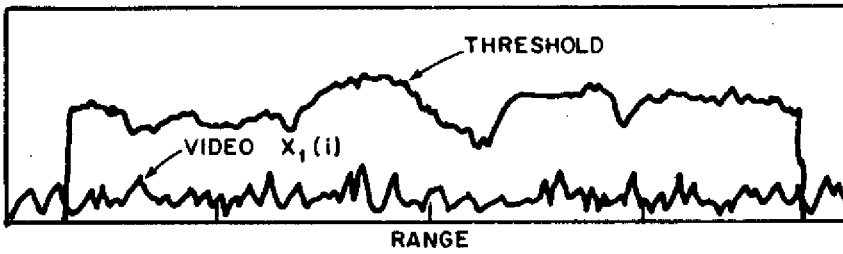


(d) Mean comparison

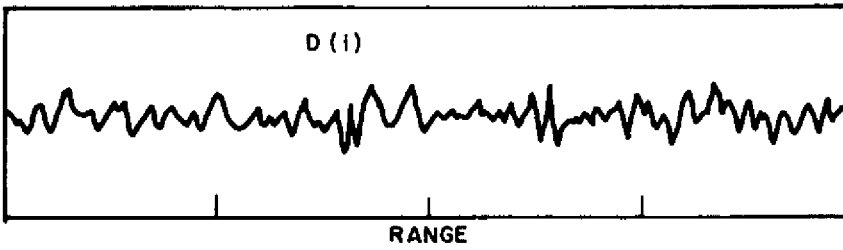
Fig. 4 - Rain clutter



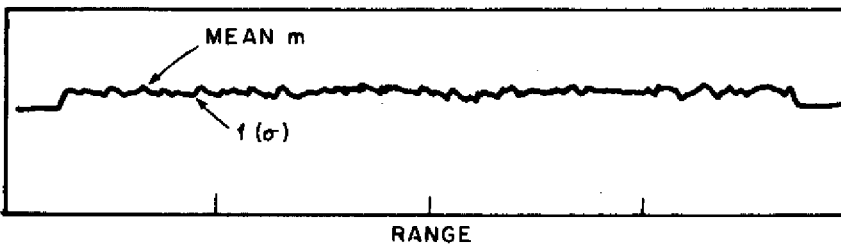
(a) Echo from pulse 1



(b) Echo from pulse 2



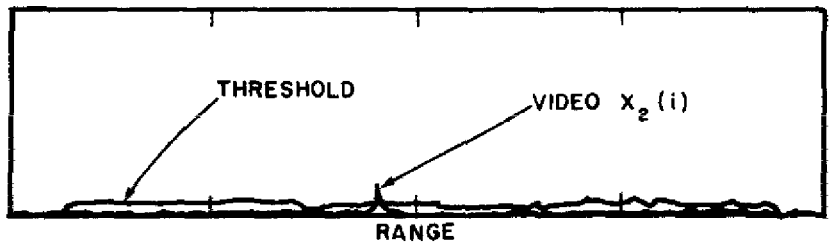
(c) Difference in echoes



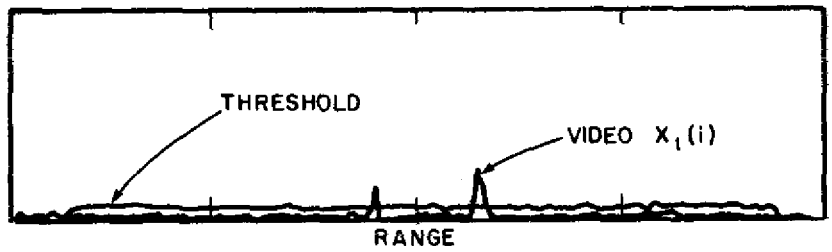
(d) Mean comparison

Fig. 5 — Noise jamming

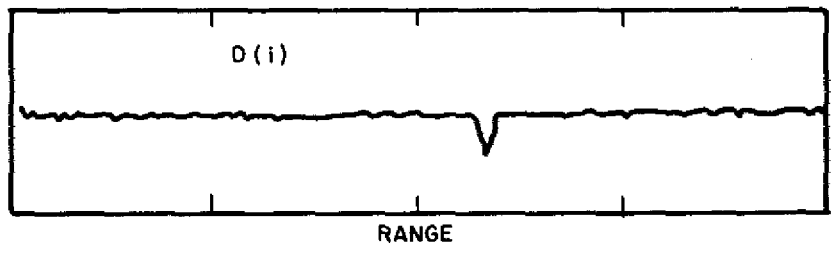
CANTRELL



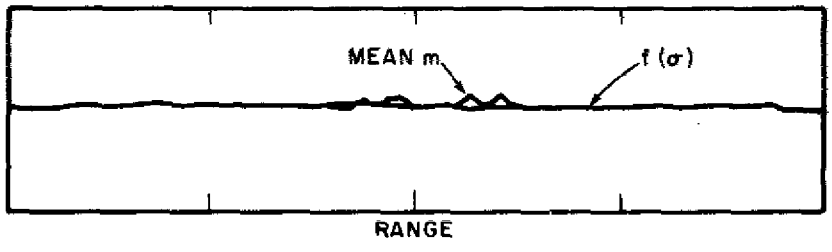
(a) Echo from pulse 1



(b) Echo from pulse 2



(c) Difference in echoes



(d) Mean comparison

Fig. 6 - Interference

deviations in the pulse echoes $X_1(i)$ and $X_2(i)$. Finally Fig. 6c shows the residue interference spikes in the $\{D(i)\}$ record which is also present in the pulse echo $X_1(i)$.

After the pulse-to-pulse correlated components have been removed, leaving the record $\{D(i)\}$, the interference spikes are detected, so that a declaration of interference can be made and so those range cells containing interference spikes can be discarded from the calculation of the threshold. The interference detector chosen is a classic log Rayleigh detector which computes

$$\log \left(10 |D(i)| + 1 \right) - \frac{1}{(N_I - 1)} \sum_{j=2}^{N_I} \log \left[10 |D(i-j)| + 1 \right] \\ - \frac{1}{(N_I - 1)} \sum_{j=2}^{N_I} \log \left[10 |D(i+j)| + 1 \right],$$

where $(N_I - 1)$ is the number of reference cells on each side of the test cell. If this number is greater than a threshold, a target is declared. This detector is equivalent to requiring that test cell $D(i)$ be a certain value above the geometric mean computed from reference cells surrounding the test cell. Adjacent range cells $D(i+1)$ and $D(i-1)$ are not used in the calculation and are sometimes referred to as guard cells. The reason this detector was chosen is that it exhibits good CFAR properties for Rayleigh-distributed noise and suffers less suppression properties than many of the other detectors [2].

The mean μ and standard deviation σ are next computed from range cells on each side of the test cell using the data record $\{D(i)\}$. The records $\{D(i)\}$ in Figs. 2 through 6 show that the mean value μ averaged over range will be small and the standard deviation formed from a range interval is proportional to the standard deviation of the uncorrelated signals in the records $X_1(i)$ and $X_2(i)$. The exception to this observation is when an interference spike is present in the $D(i)$ record and is obviously a member of a different statistical distribution. Consequently the range cells in which interference spikes have been detected are excluded from being used in the calculation of μ , σ , and $f(\sigma)$, which are defined subsequently.

The estimate of the standard deviation σ , which is proportional to the uncorrelated signals in the records $X_1(i)$ and $X_2(i)$, is compared to the standard deviation σ_n of the thermal noise as shown in Fig. 1. Examples of cases when $\sigma \gg \sigma_n$ are shown in Figs. 4 and 5, with rain and noise jamming being declared respectively. The estimate of the standard deviation of the thermal noise is obtained when no rain or jamming is present.

The next step is to detect signals which are correlated from pulse to pulse and are above the uncorrelated noise level. The threshold is computed from μ and σ , which are estimates of the mean and standard deviation of the uncorrelated noise in the local vicinity as shown in Fig. 1. Both echoes $X_1(i)$ and $X_2(i)$ are compared to the threshold, and if both

exceed the threshold, either land clutter or an isolated target is declared. The reason for the requirement of coincidence is that interference is rejected but land clutter and targets will be passed. Examples of land clutter and targets are given in Figs. 2 and 3. In Fig. 2 both targets are above the threshold derived from $\{D(i)\}$ on both echoes $X_1(i)$ and $X_2(i)$. Figure 3 shows a substantial number of detections in the heavy land clutter.

The next step in the procedure is to separate the isolated targets from the land clutter. The distinction is that isolated targets are surrounded by several range cells of uncorrelated noise whereas the land clutter is more distributed. As a digression here, it is pointed out that the probability density for the subtraction y of two independent and identically distributed Rayleigh variate whose underlying Gaussian distribution has a standard deviation of σ_g is, as described in Ref. 3, given by

$$p(y) = \frac{e^{-z^2}}{2\sigma_g^2} \left[|z| e^{-z^2} + \frac{\sqrt{\pi}}{2} (1 - 2z^2) (1 - \operatorname{erf} |z|) \right], \quad (1)$$

where $z = y/2\sigma_g$ and

$$\operatorname{erf}(z) = \frac{2}{\sqrt{\pi}} \int_z^\infty e^{-\mu^2} d\mu.$$

The density $p(y)$ has zero mean and standard deviation of $\sigma = 0.926\sigma_g$. For uncorrelated noise in the records $X_1(i)$ and $X_2(i)$, the probability density of the record $\{D(i)\}$ closely approximates the density given by Eq. (1). The estimate of the mean value in the records $X_1(i)$ and $X_2(i)$ can be found by first estimating the standard deviation of the underlying Gaussian process $\sigma_g = \sigma/0.926$ and then determining the mean of the Rayleigh distribution formed from the Gaussian as

$$f(\sigma) = (\sqrt{\pi}/2) \sigma/0.926.$$

The mean value m of the records $X_1(i)$ and $X_2(i)$ is found directly using two range cells on each side of the test cell plus a guard cell. If this mean value is near the value of $f(\sigma)$, which is the estimate of the mean after pulse-to-pulse subtraction, the region is declared an uncorrelated noise region and any correlated signal detection is allowed to be declared a target detection as shown in Fig. 1. The target detection is also subtracted from the detection of correlated signals. When the echoes $X_1(i)$ and $X_2(i)$ are correlated, $f(\sigma)$ does not change significantly, because the correlation has been removed by pulse-to-pulse subtraction, but the mean value obtained directly from the records $X_1(i)$ and $X_2(i)$ becomes large. Correlated signals are not allowed to be declared target detections under this condition and consequently are declared as land clutter.

Examples of the behavior of $f(\sigma)$ and m for various conditions are shown in part d of Figs. 2 through 6. The examples show that $f(\sigma)$ and m are nearly the same except for small regions corrupted by targets and for land clutter, given in Fig. 3d. Even though a large number of detections are obtained for the land-clutter echoes, as shown in Figs. 3a and b,

they will not be declared as isolated targets because the mean is much larger than $f(\sigma)$. In Fig. 2 the two targets are above the thresholds and will be declared as isolated targets, because the mean and $f(\sigma)$ are nearly equal in that range cell. The value of the mean m is greater than $f(\sigma)$ for a few range cells. The targets are corrupting the estimate of the mean in these cases. This becomes a problem only when the targets are closer together than three range cells.

In some cases a number of objects which should be declared land clutter can be declared as isolated targets. For example, items such as towers, isolated buildings, and bridges can provide a targetlike appearance due to their geographic location with respect to the radar. In these cases the objects can be tracked from scan to scan and be declared point clutters based on their relative motion with respect to the observer.

The last category to be described is thermal noise. Thermal noise is declared if no other declarations are made. This is as important as all the other designations, because at least in the absence of jamming a large portion of the geographic region surveyed by radars is limited to thermal noise, and this knowledge can be very useful in the tracking system.

Several comments will now be made about some of the other categories of signals and other techniques which may be useful but which are not considered in this study. If a moving target plus clutter is present, a signal fluctuation will occur in that range cell. If the fluctuation is large, it will be detected at the output of the interference declaration line. If enough pulses on target are obtained, the range cell will contain a number of interference declarations which is uncharacteristic of interference and consequently a moving target plus clutter can be declared. Another way of accepting an interference declaration in a range cell as a moving-target-plus-clutter declaration is that the region has been declared a clutter region and is essentially interference free. Another category not considered but relevant in the data collected was receiver saturation. When this occurred, the statistics changed and many of the underlying assumptions were no longer true. For these cases receiver saturation needs to be detected and all results disallowed for a few range cells surrounding the saturated conditions, which in effect is a loss of information. Considerably more is involved in considering environmental maps than considered here. However, this report will stay within the limited guidelines set forth and next present some qualitative types of results which were obtained.

QUALITATIVE RESULTS

Examples of the performance of the environmental mapping results will be displayed in a qualitative way using a PPI presentation. Echoes from the radars were recorded as they rotated in azimuth, and five range-azimuth patches of thresholded video are displayed in Fig. 7. The categories are interference and target, land clutter, two closely spaced targets, sidelobe noise jamming and a target, rain clutter, and the thermal noise regions, which are essentially the white areas.

The environmental data displayed in Fig. 7 are processed, and the interference detections are shown in Fig. 8. An excellent job of detecting the interference spikes was achieved. None of the targets or land clutter shown in Fig. 7 were declared interference. All the

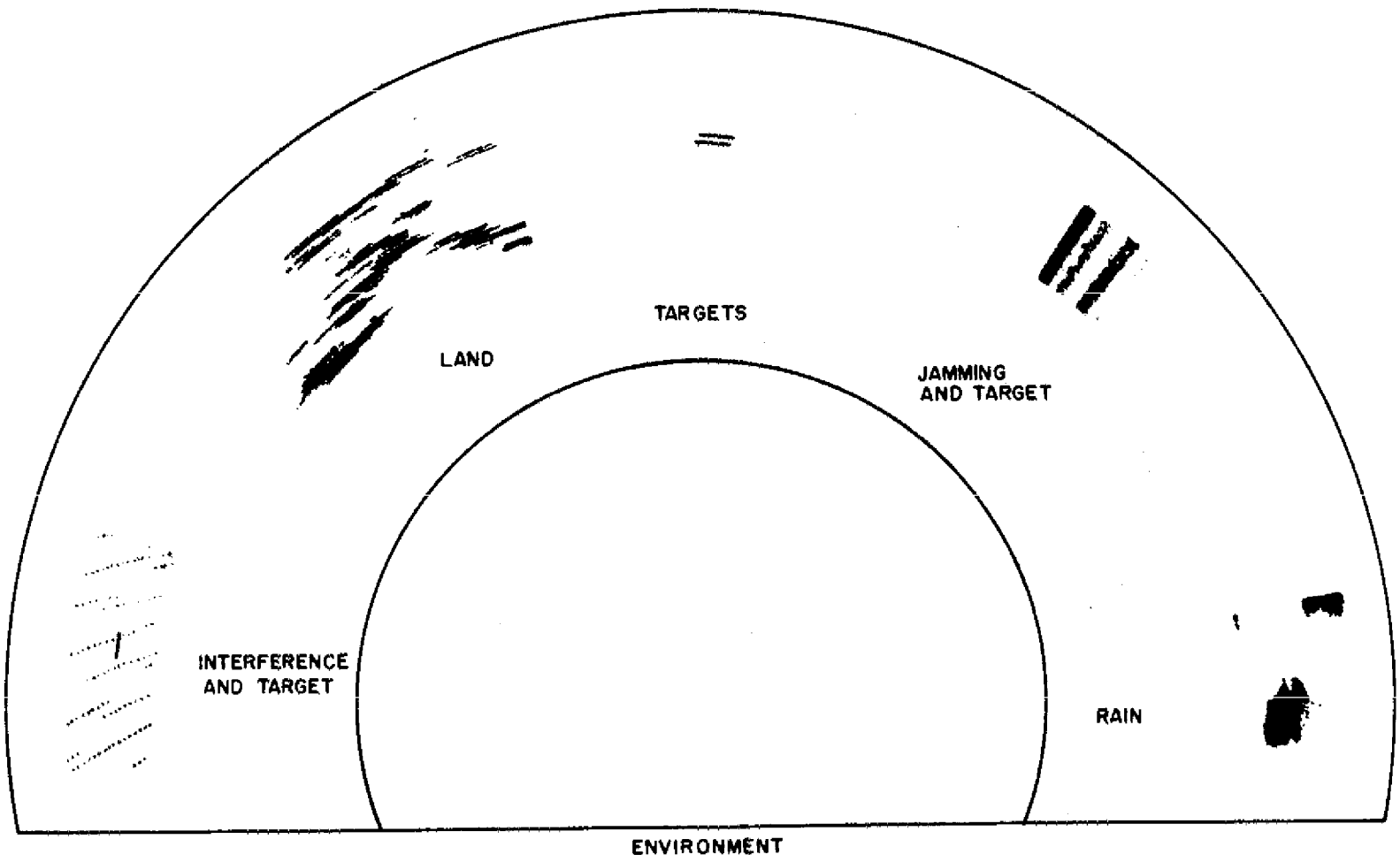


Fig. 7 — PPI representation of the environment

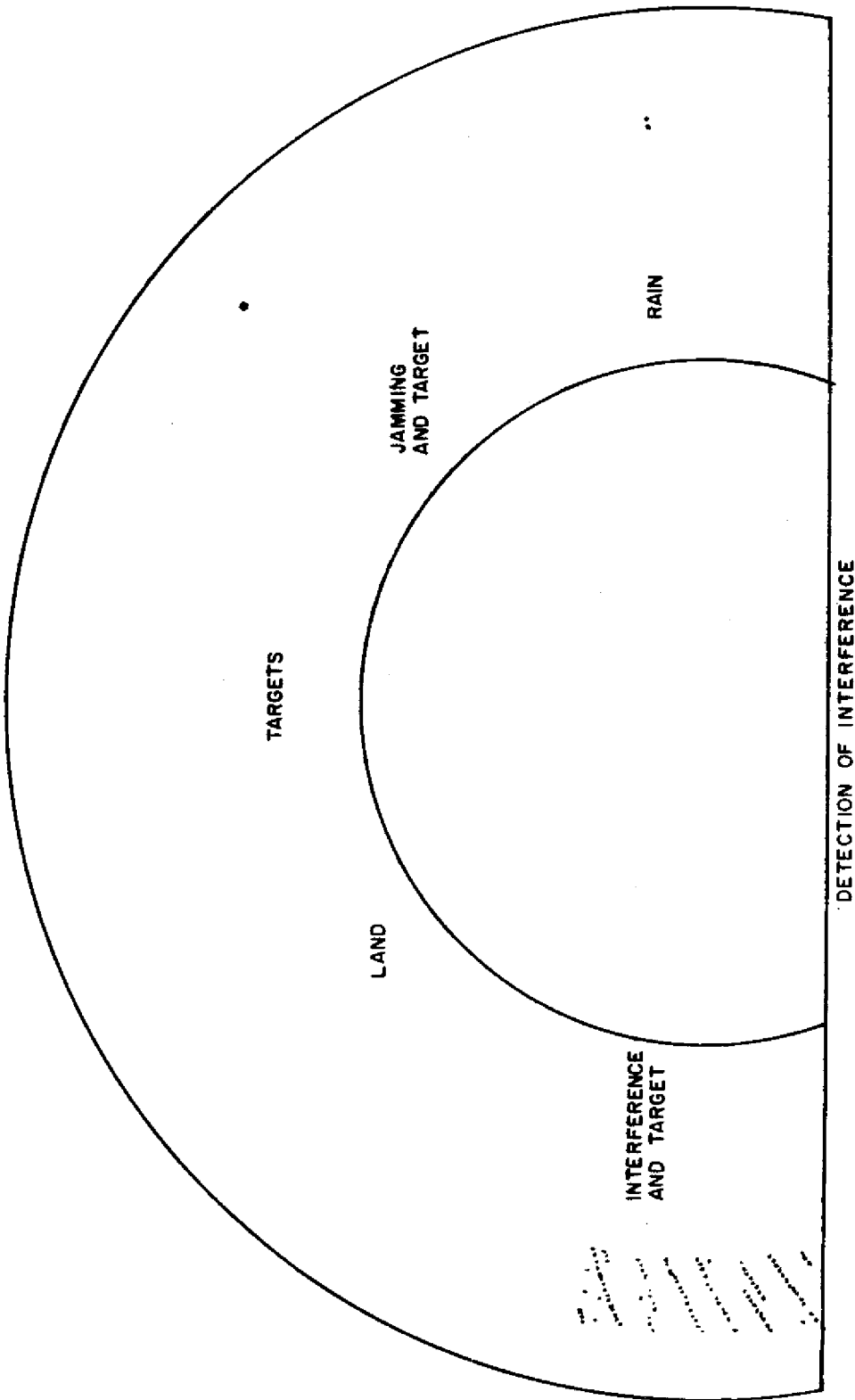


Fig. 8 — PPI representation of the detection of short pulse interference

interference spikes except three very weak ones were declared interference. A couple of interference declarations were made in the rain cloud. This occurred because of receiver saturation; consequently, when that category becomes instrumented (not described in this report), the declaration of interference in the rain cloud will no longer be present. The last item considered is the single interference declaration in the noise jamming plus target. The reason this occurred is as follows. The time between echoes was 6 ms rather than 2 ms as in all the other data, and only a few pulses on a very weak target were obtained as the beam swept over it. Because of the large scanning modulation which was not present on the other data, the weak target changed amplitude by a substantial percentage from one pulse to the next. Therefore one of these echo pairs was declared an interference spike. Although the target was weak, it was verified to be a target by examining from scan to scan the raw video return and noting that the weak target echoes were moving at nearly a constant rate.

By use of the test data in Fig. 7, the results for detecting rain and noise jamming is shown in Fig. 9. The results were good in that the rain-cloud and noise-jamming strobes were detected and no false detections were made for the target cases and land clutter. Three interference spikes were declared as jamming or rain. This occurred because the three interference spikes were low in amplitude and were not properly detected as interference spikes. Consequently they appear as uncorrelated noise but at a higher level than the general background and are declared as noise jamming or rain. The next level of mapping not considered here would consider if these detections are strobefike for noise jamming, cloudlike for rain, and pointlike for low-level interference spikes.

By use of the test data in Fig. 7, the results for detecting the land clutter is shown in Fig. 10. The results were excellent in that the land clutter was declared correctly and targets, interference, jamming, and all but one range cell in the rain cloud were not declared as land clutter. The false alarm in the rain cloud was again due to receiver saturation as mentioned earlier and consequently would not be present when the saturation category is included in the map.

By use of the test data in Fig. 7, the results for detecting the isolated targets are shown in Fig. 11. A perfect performance was achieved in that the target in the interference, the two closely spaced targets, and the weak target in the jamming mentioned earlier were all detected and no false declarations were made.

SUMMARY

Preliminary results concerning radar environmental mapping were presented. The object was to devise simple circuits, which could operate at the high data rate of the radars, that would adequately describe the signals received by the radars. In general these circuits must be tailored to each specific radar. However, for this preliminary study, data were collected and used from both L-band and S-band radars pulsed at a low pulse repetition frequency and which retained the same frequency for at least two successive pulses. The classifications of signals considered were interference, land clutter, targets, noise jamming, rain clutter, and thermal noise. The results obtained using recorded data were excellent in that the signals were classified into the correct category in almost every case and only a few false declarations were made.

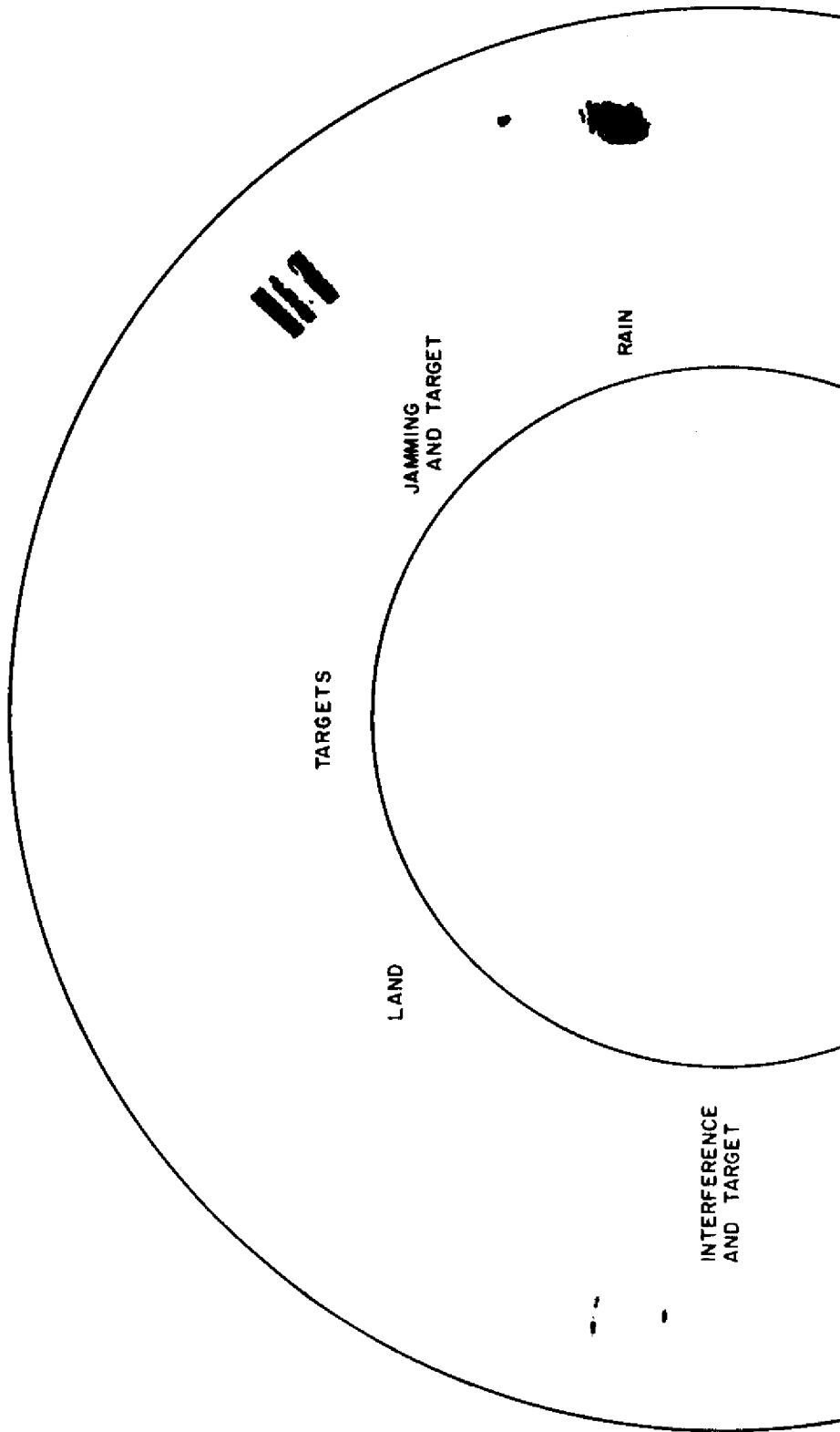


Fig. 9 — PPI representation of the detection of pulse-to-pulse uncorrelated signals

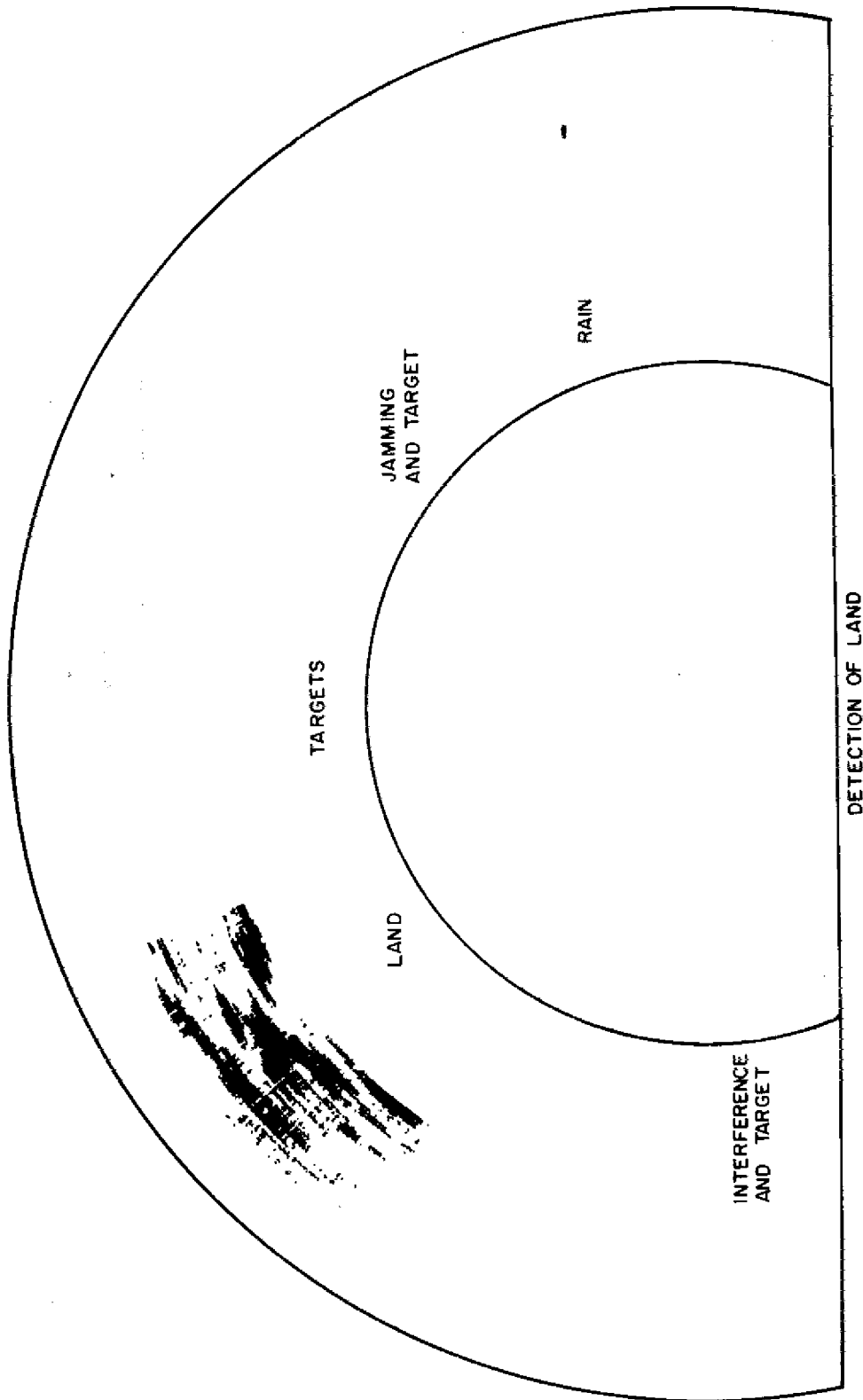


Fig. 10 — PPI representation of the detection of distributed pulse-to-pulse correlated signals

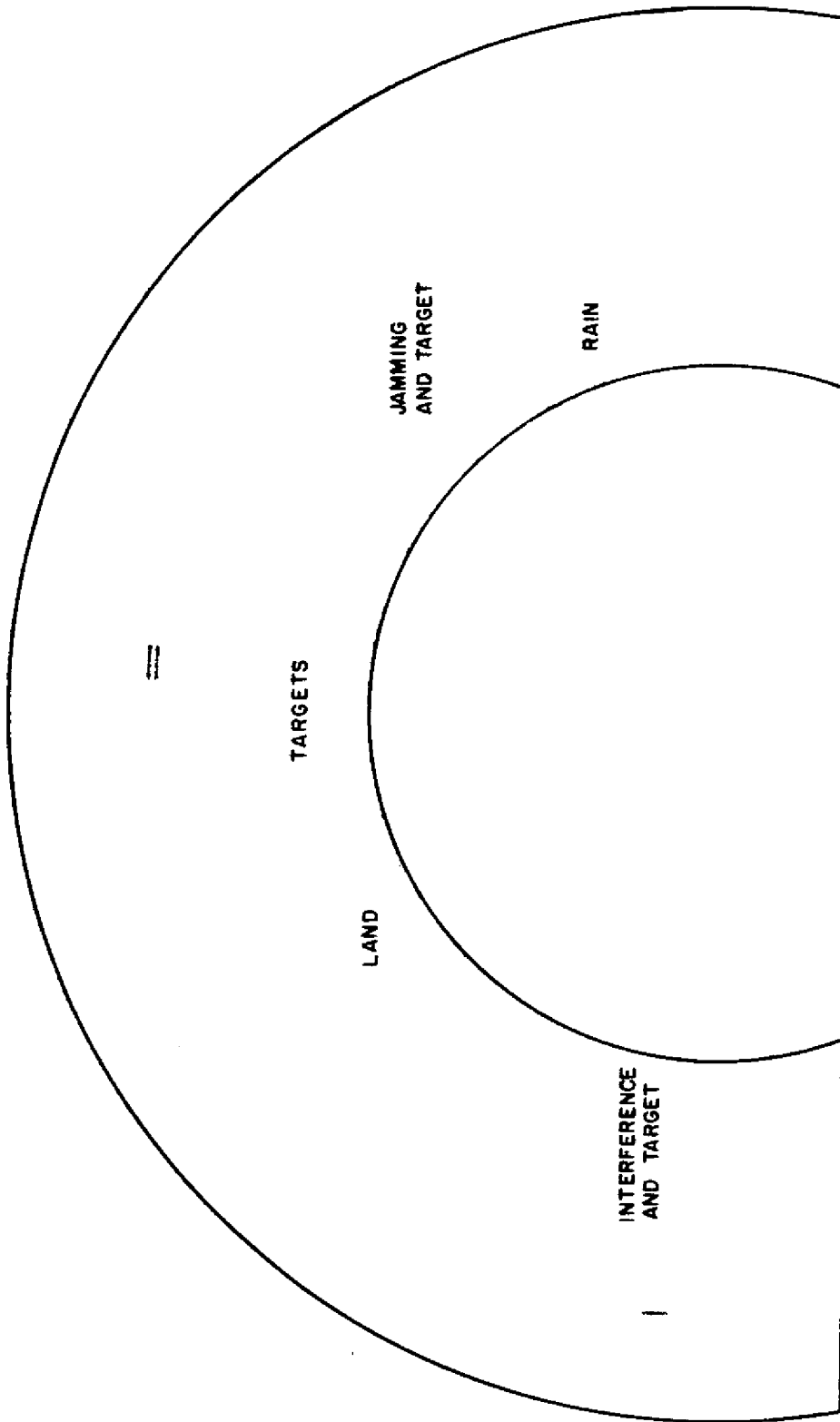


Fig. 11 — PPI representation of the detection of isolated targets

CANTRELL

This study is considered preliminary, because many aspects of the mapping were not considered. Future work may address some of the remaining problems: More signal categories should be added. More signal combinations should be studied. A regional environmental map should be constructed based on the range-cell-by-range-cell declarations described in this text. The interactions of the environmental map and the tracking system should be studied, and possibly the environmental map and tracking system should be merged so that detection and tracking are almost indistinguishable. Finally the use of environmental maps to control the radar should be considered.

ACKNOWLEDGMENTS

I thank Don Queen and Jim Alter for patiently collecting a sizable number of data. I also thank Nathan O'Neal for providing the jamming signals for the radar.

REFERENCES

1. B.H. Cantrell, "Environmental Map (High-Speed Processing Portion)," NRL patent application, Oct. 30, 1979.
2. G.V. Trunk, "Range Resolution of Targets Using Automatic Detectors," IEEE Trans. on Aerospace and Electronic Systems AES-14 (No. 5), 750-755 (Sept. 1978).
3. B.H. Cantrell, "A Short-Pulse Area MTI," NRL Report 8162, Sept. 22, 1977.